PRAMANA
— journal of
physics

Vol. 76, No. 3
March 2011
pp. 501–511

Plasma-filled rippled wall rectangular backward wave oscillator driven by sheet electron beam

A HADAP[1,*], J MONDAL[2], K C MITTAL[2] and K P MAHESHWARI[3]
[1]General Engineering Department, Terna College of Engineering, Mumbai 400 706, India
[2]Accelerator and Pulse Power Division, Bhabha Atomic Research Centre, Trombay, Mumbai 400 085, India
[3]School of Physics, Devi Ahilya University, Khandwa Road, Indore 452 167, India
*Corresponding author. E-mail: arti_99@yahoo.com; arti5_99@yahoo.com

MS received 23 December 2009; revised 4 August 2010; accepted 13 August 2010

Abstract. Performance of the backward wave oscillator (BWO) is greatly enhanced with the introduction of plasma. Linear theory of the dispersion relation and the growth rate have been derived and analysed numerically for plasma-filled rippled wall rectangular waveguide driven by sheet electron beam. To see the effect of plasma on the TM_{01} cold wave structure mode and on the generated frequency, the parameters used are: relativistic factor $\gamma = 1.5$ (i.e. $v/c = 0.741$), average waveguide height $y_0 = 1.445$ cm, axial corrugation period $z_0 = 1.67$ cm, and corrugation amplitude $\varepsilon = 0.225$ cm. The plasma density is varied from zero to 2×10^{12} cm^{-3}. The presence of plasma tends to raise the TM_{01} mode cut-off frequency (14 GHz at 2×10^{12} cm^{-3} plasma density) relative to the vacuum cut-off frequency (5 GHz) which also causes a decrease in the group velocity everywhere, resulting in a flattening of the dispersion relation. With the introduction of plasma, an enhancement in absolute instability was observed.

Keywords. Sheet electron beam; backward wave oscillator; plasma.

PACS Nos 41.85.Lc; 41.85.Ja; 52.30.Bt

1. Introduction

The backward wave oscillator is a device designed to efficiently convert the energy of an electron beam into electromagnetic radiation at microwave frequencies [1]. Emerging needs for high power and higher efficiency microwave generating devices lead to a lot of modifications in the design of backward wave oscillators. Conventional BWOs using cylindrical solid or annular beams to generate microwaves promise to be a good high-power rf (radiofrequency) source at moderate radiofrequency. But there are some limitations in carrying input power inside the slow wave structure and so the resultant power cannot be increased after some limits. The maximum current carried by the beam is

determined by the beam waveguide geometry in the interaction region. For an infinitely thin annular beam of radius r_b in a drift tube of radius r_w, the space charge limited current is

$$I_{sc} = \frac{8500(\gamma_{inj}^{2/3} - 1)^{3/2}}{\ln(r_w/r_b)}.$$

A finite thickness annular beam carries a somewhat smaller current than that given above. The space charge limiting current for a thin beam of width W located between two symmetrically placed conducting boundaries separated by a distance S is

$$I_{sc} = \frac{8500(\gamma_{inj}^{2/3} - 1)^{3/2} W}{2\pi S}.$$

For a length of sheet beam about one half of the circumference of the annular beam, one may achieve comparable impedance operation. The factor of $2(r_w - r_b \cong s)$ arises from the fact that the sheet beam fields extend equally to either waveguide plate. This factor of 2 in the current density may be significant when bunching is important. More significant however, is the point that high beam currents are achieved when the beam is located on the axis of symmetry of the system, that is, at the peak axial field location for a TM_{01} mode. It is possible to produce sheet beams with 1–2 mm thickness and widths up to 50 cm provided that instabilities can be controlled, whereas in the case of annular beams, the beam current depends not on the size of the drift tube but on the ratio of the beam to waveguide radius. In practice, some limitations arise, principally due to the finite thickness of the beam, which is difficult to reduce below 1–2 mm. Limiting currents of about one-third of the value given above are common in small tubes, whereas one can approach the full limiting current in larger tubes where the beam width is small compared to its radius. The beam current can be made large in the case of annular beam if a thin beam is generated close to the waveguide wall, and for a fixed thickness beam scales linearly with the tube radius. Unfortunately, the beam location is frequently fixed at a given fraction of the tube radius for efficient coupling to the wave. For example, in the coupling to a TE_{01} mode it is desirable to have the beam located at about half the tube radius. Because of the above limitations, here we are considering the model of microwave generation as a rectangular waveguide driven by sheet electron beam.

Recent research has demonstrated that the presence of controlled amounts of plasma inside microwave sources can in many cases dramatically improve the tube performance compared to vacuum devices. Plasma filling has been used in a variety of sources, including backward wave oscillator (BWO travelling wave tube (TWT) amplifiers, gyratrons and other microwave tubes), to increase the overall efficiency gain, frequency bandwidth, maximum electron beam current and in some cases to reduce the need for guiding magnetic fields.

In this paper we study the effect of sheet beams in plasma-filled waveguide on growth rate and hence on the output power. The practical measure of the strength of instability is the spatial growth rate [2] rather than the temporal growth rate because in linear theory the output radiation is proportional to $\exp(i\omega t)$, where t is the interaction time between

the beam and the backward wave. In real experiments, the interaction time $t \gg 1$ ns is the ratio of finite length L of the guide to group velocity. Then $\exp(i\omega t) = \exp(ikL) \gg 1$. The increase in *im*(k) with plasma density is presented.

In our study we have chosen a rectangular rippled slow wave structure (SWS) [3]. The wall height y_w of the waveguide varies sinusoidally according to the relation, $y_w = y_0 + \xi \cos(k_w z)$, where $k_w = 2\pi/D$, D is the spatial periodicity, y_0 is the mean radius and ξ is the modulation amplitude. A uniform, cold and collisionless plasma with density N_p is assumed to be present, and a beam with uniform electron density N_b, a longitudinal velocity v_b and height $\Delta < y_0$ is also present in the SWS. Recently, introduction of plasma from the external gun in the SWS shows considerable increase in both the output power and the efficiency [4]. This paper is devoted to a comprehensive theoretical treatment of the interaction of rectangular rippled BWO driven by sheet electron beam. Space charge effects are considerably mitigated by diluting the current density with the introduction of sheet electron beam. Here we follow the earlier investigation [5] to reduce the dispersion relation into 3×3 matrix. We study the effect of variation of filled plasma density on the dispersion curve as well as on the spatial growth rate. It is seen that with the increase in plasma density cut-off of the dispersion curve increases leading to higher frequency generation, but the group velocity decreases as well. It is also seen that there is a resonant increase in the spatial growth rate for a particular plasma density keeping other parameters unchanged. In §2, we present the dispersion relation of the plasma-filled rectangular rippled BWO driven by sheet electron beam. Section 3 contains the reduction of the dispersion relation to a manageable size. Section 4 deals with the derivation of spatial growth rate using perturbation analysis. Finally, in §5 we present the results and discussion.

2. Dispersion relation

Consider the interaction between sheet electron beam of density N_b in axially rippled infinitely long rectangular waveguide as in ref. [6]. The whole geometry of the slow wave structure (SWS) along with the sheet beam is immersed in a strong longitudinal magnetic field ideally having infinite magnitude. Under this assumption the electron motions are 1D in the axial direction and the relative dielectric tensor may be written as

$$\varsigma_r = \begin{bmatrix} 1 & 0 & 0 \\ 0 & 1 & 0 \\ 0 & 0 & \varsigma_{zn} \end{bmatrix} \tag{1}$$

and by [7]

$$\varsigma_{zn} = 1 - (\omega_p/\omega)^2 - \omega_b^2/(\gamma^3 \times (\omega - k_n v)^2), \tag{2}$$

where $\omega_p = (e^2 N_p/m_e \xi_0)^{1/2}$ is the plasma frequency and $\omega_b = (e^2 N_b/m_e \xi_0)^{1/2}$ is the beam plasma frequency.

The SWS is filled with a cold, homogeneous, collisionless plasma of density N_p. We further assume that: (i) the electron cyclotron frequency should be larger than ω_p and ω_b so that the cyclotron effect do not play a role in the generation process, (ii) the beam is

monoenergetic, (iii) the waveguide wall is perfectly conducting and held at zero potential, and (iv) the beam is free from any kind of macroscopic instabilities.

We choose transverse magnetic modes (TM) because their axial electric field component drives the axial bunching of the electron beam. In mathematical terms we express the propagation field equation as $\exp\{-i[k_{\mathrm{n}}z - \omega t]\}$, following the Floquet's theorem E_y and E_x are directly proportional to $\exp(ik_n z)$, where $k_n = k_z + nk_{\mathrm{w}}$. By using the Fourier decomposition of the x, y, z-components of the wave equation we can write down the z component of the electric field as

$$E_z(y, z, t) = \sum_{n=-\infty}^{n=\infty} E_{zn} \exp(i(\omega t - k_n z)). \tag{3}$$

This equation shows that the periodicity of the SWS is a general waveguide solution in an infinite summation of spatial harmonics.

The wave equation for the z-component of electric field in the region $0 \leq y \leq \Delta/2$ is

$$\frac{\mathrm{d}^2 E_{zn}}{\mathrm{d}y^2} + p_n^2 E_{zn} = 0, \tag{4}$$

where

$$p_n^2 = (\varsigma_{zn} k_0^2 - k_n^2). \tag{5}$$

For the region $\Delta/2 \leq y \leq y_{\mathrm{w}}$, the wave equation for E_{zn} is

$$\frac{\mathrm{d}^2 E_{zn}}{\mathrm{d}y^2} + Q_n^2 E_{zn} = 0, \tag{6}$$

where

$$Q_n^2 = \left(1 - \frac{\omega_{\mathrm{p}}^2}{\omega^2}\right) k_0^2 - k_n^2. \tag{7}$$

Equations (4) and (6) lead to the solution

$$E_{zn} = a_n \cos(p_n y) + b_n \sin(p_n y), \quad 0 \leq y \leq \Delta/2, \tag{8a}$$

$$E_{zn} = c_n \cos(Q_n y) + d_n \sin(Q_n y), \quad \Delta/2 \leq y \leq y_{\mathrm{w}}. \tag{8b}$$

y-components of the electric field in the two regions are

$$E_{yn} = -\frac{jk_n}{p_n^2}\left[-a_n p_n \sin(p_n y) + b_n p_n \cos(p_n y)\right], \quad 0 \leq y \leq \Delta/2 \tag{9a}$$

and

$$E_{yn} = -\frac{jk_n}{Q_n^2}\left[-c_n Q_n \sin(Q_n y) + d_n Q_n \cos(Q_n y)\right], \quad \Delta/2 \leq y \leq y_{\mathrm{w}}. \tag{9b}$$

The vertical symmetry of the beam along with SWS lead to $E_{yn} = 0$ at $y = 0$.

Applying the above condition to y- and z-components of the electric field in the region $0 \leq y \leq \Delta/2$, gives us $b_n = 0$.

Hence

$$E_{yn} = \frac{jk_n}{p_n} a_n \sin(p_n y), \quad 0 \leq y \leq \Delta/2, \tag{10}$$

$$E_{zn} = a_n \cos(p_n y), \quad 0 \leq y \leq \Delta/2. \tag{11}$$

Now, applying the matching condition at $y = \Delta/2$ to the y- and z-components of the electric field and after some straightforward mathematics we arrived at the following relations:

$$c_n = a_n T_n, \tag{12}$$

where

$$T_n = a_n \left[\cos(Q_n \Delta/2)\cos(p_n \Delta/2) + (p_n/Q_n)\sin(Q_n \Delta/2)\sin(p_n \Delta/2)\right] \tag{13}$$

and

$$d_n = a_n L_n, \tag{14}$$

where

$$L_n = a_n \left[\sin(Q_n \Delta/2)\cos(p_n \Delta/2) - (p_n/Q_n)\cos(Q_n \Delta/2)\sin(p_n \Delta/2)\right]. \tag{15}$$

Finally we have

$$E_{zn} = a_n T_n \cos(Q_n y) + a_n L_n \sin(Q_n y), \quad \Delta/2 \leq y \leq y_{\mathrm{w}}. \tag{16}$$

Here we have used the Floquet's theorem to account for periodicity in z. Using the boundary condition of vanishing the tangential component of the electric field on the boundary of the electric field on the surface of the metallic wall, we have

$$E_z(y_{\mathrm{w}}) + E_y(y_{\mathrm{w}}) \frac{\mathrm{d}}{\mathrm{d}z} y_{\mathrm{w}} = 0, \tag{17}$$

i.e.,

$$\sum_{n=-\infty}^{n=\infty} \left[E_{zn}(y_{\mathrm{w}}) - \frac{jk_n}{h_n^2} \frac{\mathrm{d}}{\mathrm{d}z} E_{zn}(y_{\mathrm{w}}) \right] = 0. \tag{18}$$

To eliminate the axial dependence, we follow Kurliko *et al* [7] and multiply by $\mathrm{e}^{jk_m z}$ and axially integrate from $z = -D/2$ to $D/2$. This gives

$$0 = \sum_{n=-\infty}^{n=\infty} \int_{-D/2}^{D/2} \mathrm{d}z\, \mathrm{e}^{j(k_m - k_n)z} \left(1 - \frac{jk_n}{h_n^2} \frac{\mathrm{d}}{\mathrm{d}z}\right) \times \{a_n T_n \cos(Q_n y) + a_n L_n \sin(Q_n y)\} \tag{19}$$

or

$$0 = \sum_{n=-\infty}^{n=\infty} \int_{-D/2}^{D/2} \mathrm{d}z\, \mathrm{e}^{j(k_m-k_n)z} \{a_n T_n \cos(Q_n y) + a_n L_n \sin(Q_n y)\} + \sum_{n=-\infty}^{n=\infty} \int_{-D/2}^{D/2} \mathrm{d}z\, \mathrm{e}^{j(k_m-k_n)z} \left(-\frac{jk_n}{h_n^2}\frac{\mathrm{d}}{\mathrm{d}z}\right) \times \{a_n T_n \cos(Q_n y) + a_n L_n \sin(Q_n y)\}. \quad (20)$$

After integrating the second term by parts we find

$$0 = \sum_{n=-\infty}^{n=\infty} \int_{-D/2}^{D/2} \mathrm{d}z\, \mathrm{e}^{j(k_m-k_n)z} \{a_n T_n \cos(Q_n y) + a_n L_n \sin(Q_n y)\} + \sum_{n=-\infty}^{n=\infty} \left[\mathrm{e}^{j(k_m-k_n)z} \left(-\frac{jk_n}{h_n^2}\right) \{a_n T_n \cos(Q_n y) + a_n L_n \sin(Q_n y)\}\right]_{-D/2}^{+D/2} + \sum_{n=-\infty}^{n=\infty} \int_{-D/2}^{D/2} \mathrm{d}z - (k_m - k_n)\, \mathrm{e}^{j(k_m-k_n)z} \left(\frac{k_n}{h_n^2}\right) \times \{a_n T_n \cos(Q_n y) + a_n L_n \sin(Q_n y)\}. \quad (21)$$

The middle term vanishes at the end points (the sine terms are identically zero and the cosine terms cancelled) and we can rewrite the boundary condition as

$$0 = \sum_{n=-\infty}^{n=\infty} a_n \int_{-D/2}^{D/2} \mathrm{d}z\, \mathrm{e}^{j(k_m-k_n)z} \frac{\left[k_0^2 - k_m k_n\right]}{h_n^2} \times \{T_n \cos(Q_n y) + L_n \sin(Q_n y)\}. \quad (22)$$

The above equation is of the form

$$\overleftrightarrow{D} \cdot \vec{A} = 0, \quad (23)$$

where $\overleftrightarrow{D}$ and $\vec{A}$ are matrices with, $\vec{A} = (..., a_{-n}, ..., a_{-1}, a_1, ..., a_n, ...)^{\mathrm{T}}$. In order to have a nontrivial solution, the determinant $\overleftrightarrow{D}$ must be zero, which is the dispersion relation.

3. Cold structure mode dispersion

To derive the functional relationship between frequency generated and wave number at this point in the dispersion relation (22), we assume that beam density is infinitesimally small ($\omega_{\mathrm{b}} = 0$). In this case $p_n^2 = Q_n^2$ from eqs (5) and (7), $T_n = 1$ and $L_n = 0$ from eqs (13) and (15). Now eq. (22) reduces to

$$0 = \sum_{n=-\infty}^{n=\infty} a_n \int_{-D/2}^{D/2} \mathrm{d}z\, \mathrm{e}^{j(k_m-k_n)z} \frac{\left[k_0^2 - k_m k_n\right]}{h_n^2} \cos(Q_n y). \quad (24)$$

Our next assumption is that the ripple amplitude is small ($\xi \ll 1$), so that we can expand the argument in eq. (24) and get a simpler form of the dispersion relation

$$\cos(Q_n y_w) = C_n - \frac{\psi Q_n y_0}{2} S_n \left(e^{jk_w z} + e^{-jk_w z}\right). \tag{25}$$

Here, $\psi = \xi/y_0$, $C_n = \cos(Q_n y_0)$ and $S_n = \sin(Q_n y_0)$.

Using eq. (25), eq. (24) reduces to

$$0 = \sum_{n=-\infty}^{\infty} a_n \frac{k_0^2 - k_n k_m}{h_n^2} \left\{ \delta_{m,n} C_n - \left(\delta_{m+1,n} + \delta_{m-1,n}\right) S_n \frac{\psi Q_n y_0}{2} \right\}. \tag{26}$$

We can rewrite eq. (26) as a homogeneous matrix equation

$$D \cdot A = 0, \tag{27}$$

where A is a vector with the elements a_n and D is a matrix with the elements

$$D_{m,n} = \frac{k_0^2 - k_n k_m}{h_n^2} \left\{ \delta_{m,n} C_n - \left(\delta_{m+1,n} + \delta_{m-1,n}\right) S_n \frac{\psi Q_n y_0}{2} \right\}, \tag{28}$$

where

$$\delta_{m,n} = \int_{-D/2}^{D/2} e^{j(k_m - k_n)z} \quad \text{and} \quad \delta_{m+1,n} = \int_{-D/2}^{D/2} e^{j(k_m - k_n + k_w)z},$$
$$\delta_{m-1,n} = \int_{-D/2}^{D/2} e^{j(k_m - k_n - k_w)z}.$$

Now, for the cold structure dispersion relation as a result, in eq. (27), A be nontrivial (i.e. at least some $A_n \neq 0$) so the determinant of D must vanish,

$$\det[\mathrm{D}] = 0. \tag{29}$$

Equation (29) is the desired cold structure dispersion relation involving the system parameters and explicitly linking α and k_z. Although eq. (29) involves an infinite matrix in principle, in practice we truncate it to some manageable size. For small ripple amplitude we confined ourselves for Floquet's harmonic corresponding to $-1 \leq m,\ n \leq 1$ of eq. (28) and we were left with the 3×3 matrix. On that basis the elements of D matrix are

$$D = \begin{pmatrix} C_{-1} & S_0 \frac{\psi Q_0 y_0}{2} \frac{k_0^2 - k_z k_{-1}}{h_0^2} & 0 \\ S_{-1} \frac{\psi Q_{-1} y_0}{2} \frac{k_0^2 - k_{-1} k_z}{h_{-1}^2} & C_0 & S_1 \frac{\psi Q_1 y_0}{2} \frac{k_0^2 - k_z k_1}{h_1^2} \\ 0 & -S \frac{\psi Q_0 y_0}{2} \frac{k_0^2 - k_z k_1}{h_0^2} & C_1 \end{pmatrix} \tag{30}$$

and finally we arrived at a dispersion relation for small variation of ripple amplitude

$$C_{-1}C_0C_1 + \frac{\psi^2 Q_0 Q_1 y_0^2}{4h_0^2}\left[S_0S_{-1}C_{-1}\frac{\left(k_0^2 - k_1k_z\right)^2}{h_1^2} - S_0S_{-1}C_1\frac{\left(k_0^2 - k_zk_{-1}\right)^2}{h_{-1}^2}\right] = 0. \tag{31}$$

By substituting the value of waveguide parameters and plasma density, a relationship can be obtained between the wave number (k_z) and frequency (ω). The results for the above dispersion relation are shown in §5.

4. Spatial growth rate

Spatial growth rate is found to be a more practical measure of the strength of instability, and so to calculate that spatial growth rate here we assume sheet electron beam, viz. beam height is small ($\Delta/2 \ll y_0$) compared to the average height of the SWS, eqs (13) and (15) can be rewritten in the following form:

$$T_n = 1 - \frac{\eta\Delta^2}{(\omega - k_n v_\mathrm{b})^2 Q_n} \tag{32}$$

and

$$L_n = \frac{\eta\Delta}{(\omega - k_n v_\mathrm{b})^2 Q_n}, \tag{33}$$

where

$$\eta = \frac{\omega_\mathrm{b}^2 k_0^2}{2\gamma^3}. \tag{34}$$

Assuming ripple amplitude ($\xi \ll \mathrm{y}_0$) is small compared to the average height of the SWS, eq. (22) reduces to a final form for sheet electron beam

$$0 = \sum_{n=-\infty}^{\infty} a_n \frac{k_0^2 - k_nk_m}{h_n^2}\left\{\delta_{m,n}\left(C_n + L_nS_n\right) + \left(\delta_{m+1,n} + \delta_{m-1,n}\right)\left(-S_n + L_nC_n\right)\frac{\psi Q_n y_0}{2}\right\}. \tag{35}$$

In the above expression we retained the terms linear in Δ and neglected higher-order terms. Now the dispersion relation with sheet electron beam can be written for $-1 \le m$, $n \le 0$, i.e., truncating the infinite matrix to a 3×3 matrix

$$Q_{-1}Q_0\left(\omega - k_{-1}v_\mathrm{b}\right)^2\left(\omega - k_zv_\mathrm{b}\right)^2 + \eta\Delta Q_0(\omega - k_zv_\mathrm{b})^2 t_{-1} + \eta\Delta Q_{-1}\left(\omega - k_zv_\mathrm{b}\right)^2 t_0 = 0, \tag{36}$$

where

$$t_{-1} = \frac{S_{-1}}{C_{-1}} \quad \text{and} \quad t_0 = \frac{S_0}{C_0}.$$

Expanding each term in the dispersion relation (eq. (36)) about $k_z = k_r + ik_i$, where k_i is small, we arrived at a quartic equation for spatial growth rate

$$Q_{-1}Q_0 v_{\rm b}^4 k_i^4 - 2Q_{-1}Q_0 v_{\rm b}^4 k_{\rm w} k_i^3 + \left(Q_{-1}Q_0 v_{\rm b}^4 k_{\rm w}^2 + \eta\Delta Q_0 v_{\rm b}^2 t_{-1} + \eta\Delta Q_{-1} v_b^2 t_0\right)k_i^2 - \left(2\eta\Delta Q_{-1} v_{\rm b}^2 t_0 k_{\rm w}\right)k_i + \eta\Delta Q_{-1} v_{\rm b}^2 t_0 k_{\rm w}^2 = 0, \tag{37}$$

where

$$Q_{-1} = \sqrt{\left(1 - \frac{\omega_{\rm p}^2}{\omega^2}\right)k_0^2 - (k_{\rm r} - k_{\rm w})^2}, \tag{38a}$$

$$Q_0 = \sqrt{\left(1 - \frac{\omega_{\rm p}^2}{\omega^2}\right)k_0^2 - k_{\rm r}^2}, \tag{38b}$$

$$t_0 = \frac{\sin(Q_0 y_0)}{\cos(Q_0 y_0)},$$

and

$$t_{-1} = \frac{\sin(Q_{-1} y_0)}{\cos(Q_{-1} y_0)}. \tag{38c}$$

By substituting the waveguide parameters and varying the plasma density in the above equations, one can get the maximum spatial growth rate at a particular plasma frequency. The results are shown in §5.

5. Results and discussions

To get cold wave structure mode, i.e. in the absence of beam [8], we solved eq. (31) with $\omega_{\rm b} = 0$. In the absence of the source term Maxwell's equations are inherently linear and for that the dispersion relation is exact. We did our numerical calculations with the following set of numerical parameters:

$$y_0 = 1.445\,\text{cm}, \quad \xi = 0.225\,\text{cm}, \quad k_{\rm w} = 3.76\,\text{cm}^{-1},$$
$$\omega_{\rm b} = 5.15 \times 10^{10}\,\text{s}^{-1}, \quad \Delta = 0.5\,\text{cm}, \quad \gamma = 1.5.$$

Figure 1 depicts the calculated TM_{01} mode dispersion curves in a plasma-filled rectangular rippled BWO driven by sheet electron beam. We varied plasma density from $N_{\rm p} = 0 - 2 \times 10^{12}\,\text{cm}^{-3}$ and beam space charge line (assuming $\omega_{\rm b} = 0$) and the light line are superimposed on this dispersion curve. Results seen from figure 1 that the presence of the plasma tends to raise the TM_{01} mode cut-off frequency besides causing a decrease in the group velocity everywhere resulting in a flattening of the dispersion relation. To see the effect of plasma density $N_{\rm p}$ on spatial growth rate we considered $N_{\rm p}$ as a variable keeping other parameters constant. The spatial growth rate is a more practical measure

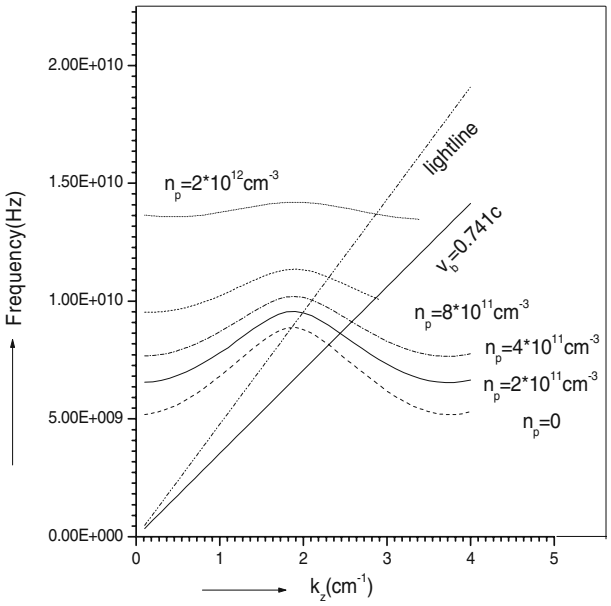

Figure 1. The calculated effect of varying the plasma density on the corrugated waveguide dispersion $y_0 = 1.445$ cm, $\xi = 0.225$ cm, $k_w = 3.76$ cm^{-1}.

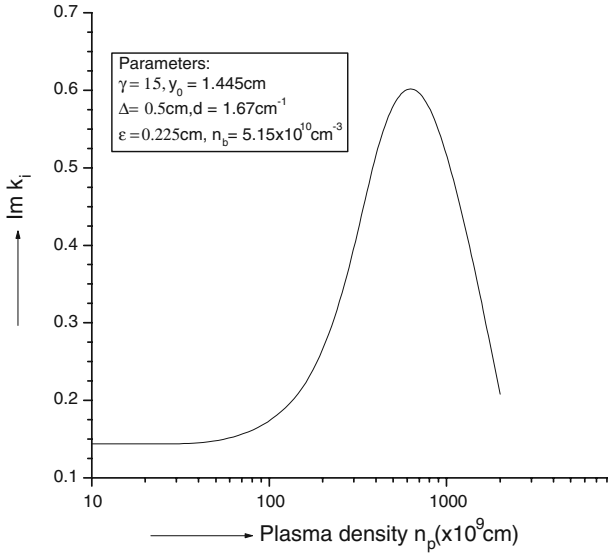

Figure 2. Variation of spatial growth rate with the variation of plasma density.

of the strength of instability than the temporal growth rate [9]. We numerically solved eq. (36) and the result is depicted in figure 2. A resonant increase in the spatial growth rate is found for plasma density which is 6×10^{11} cm^{-3}. This enhancement in the spatial growth rate can be explained from figure 2, with the increase in plasma density group velocity of the TM_{01} mode decreases leading to an enhancement in interaction between the sheet beam and the backward electromagnetic wave. This in turn leads to an enhanced microwave radiation, or in other words, a resonance in the spatial growth rate at an optimum plasma density is found.

6. Conclusion

In this paper, we have analysed theoretically and numerically the performance of a microwave source consisting of plasma-filled rectangular rippled waveguide driven by sheet electron beam guided by a strong magnetic field. An enhancement in the spatial growth rate was found. We conclude that it is possible to use sheet electron beam in a plasma-filled rectangular waveguide as a means of enhancing the total power capability in the frequency range 1 GHz to 20 GHz. Further experiments can be planned with these parameters. A particular amount of plasma density inside the cavity shows a dramatic change in the efficiency of the device. The calculation of the effect of plasma loading in the stability of sheet electron beam under diocotron instability in this new geometry is underway.

Acknowledgement

Arti Hadap would like to acknowledge with thanks the financial support provided by DST.

References

[1] J R Pierce, *Travelling wave tubes* (Van Nostrand, Princeton, NJ, 1950)
[2] M M Ali, K Minami, K Ogura, T Hosokawa, H K Azama, T Ozawa, T Watanabe, Y Carmel, V L Granststein, W W Destler, R A Khes, W R Lou and D Abe, *Phys. Rev. Lett.* **65(7)**, 855 (1990)
[3] B E Carlsten, *Phys. Plasmas* **8**, 4585 (2001)
[4] Y Carmel, K Minami, R A Khes, W W Destler, V L Granatstein, D K Abe and W L Lou, *Phys. Rev. Lett.* **62**, 2389 (1989)
[5] Y Choyal and K P Maheshwari, *Phys. Plasmas* **1**, 171 (1994)
[6] A Gokhale, J Mondal, K C Mittal, Y Choyal and K P Maheshwari, *Phys. Plasmas* (accepted for publication)
[7] V I Kurilko *et al*, *Sov. Phys.-Tech. Phys.* **26**, 812 (1981)
[8] J A Swegle, *Phys. Fluids* **28**, 2882 (1985)
[9] R J Briggs, *Electron-stream interaction with plasmas* (MIT Press, Cambridge, Mass., 1964)